Study of Precipitation Reactions by X-ray Microscopy: $CaCO_3$ Precipitation and the Effect of Polycarboxylates

J. Rieger,*,† J. Thieme,‡ and C. Schmidt‡

Polymer Physics/Solid State Physics, BASF Aktiengesellschaft, 67056 Ludwigshafen, Germany, and X-Ray Physics, University of Göttingen,Geiststrasse 11, 37073 Göttingen, Germany

Received March 20, 2000. In Final Form: August 2, 2000

A fundamental understanding of precipitation reactions is based on information about the structural evolution of the system on all length scales and starting at the beginning of the reaction. We introduce *X-ray microscopy* as an additional analytical tool in order to achieve this understanding. X-ray microscopy combines high resolution (down to 40 nm) and experiments at ambient pressure. The latter point allows the study of colloidal systems within the water phase and the performance of time-resolved microscopy. Taking $CaCO_3$ precipitation as a model system, it is shown how further knowledge can be obtained on the dynamics of structure formation. We discuss the following points: formation and recrystallization of precursors; transient stabilization of $CaCO_3$ nanoparticles by polycarboxylates; dependence of the structure evolution (stabilization or recrystallization) on the polymer concentration.

1. Introduction

Precipitation Reactions. Precipitation reactions, i.e., formation of colloidal solids from supersaturated solutions, are still far from fully understood even after more than 100 years of research. There are several aspects of the missing knowledge:

(a) In recent years, there has been an increase in the number of studies showing that processes occurring at a molecular and nanoscale level are more complex than usually assumed in the past. The classical picture of nucleation and growth often does not adequately describe the processes occurring in reality. Instead, it has now become apparent that solid-phase conversions, aggregation processes, and recrystallization phenomena during precipitation must be taken into account. In support of this thesis, we refer here by way of example to the papers by Matijevic,[1] Muramatsu,[2] Ocanja,[3] and Cölfen[4] and by ourselves.[5]

(b) In industry, precipitation reactions play a crucial role in a number of products, for example in precipitation catalysts, pigments, encrustation inhibitors, and the micronization of active ingredients. In many cases, the corresponding processes or products have been substantially optimized in empirical terms, which, especially under varying production conditions, may result in undesired changes in the product and consequently in complex experiments to find a new optimum. For this reason, industry is also interested in "understanding" precipitation reactions.

(c) In principle, precipitation reactions can be "controlled" using additives. For example, this is the basis for the success of polymeric encrustation inhibitors in detergents and in seawater desalination. These additives prevent the precipitation of low-solubility salts (for example $CaCO_3$) from the hot water on fabric surfaces and heating coils. However, the optimum additive can again only be developed if the mechanisms by which it participates in the precipitation (or crystallization) process are known. In the past, it was frequently assumed that these additives essentially develop their action through specific interaction with crystal growth surfaces. Our own studies have shown that polymeric encrustation inhibitors also interact with precipitating precursors ($CaCO_3$ nanoparticles as precursors of the crystals only formed later) at an early stage of precipitation.[5] Product optimization in the case of additives therefore again requires fundamental knowledge of structure evolution during precipitation.

However, a fundamental understanding of structure evolution in precipitation reactions is only possible if the processes can be followed from commencement of supersaturation (which initiates the precipitation) with a time resolution down to the millisecond region. To this end, corresponding analytical methods have been developed[5] which do allow fundamentally new knowledge to be obtained.

X-ray Microscopy. X-rays within the wavelength range of 0.3−5 nm are best suited for X-ray microscopy studies of colloidal systems in aqueous media. Due to this much shorter wavelength X-ray microscopy provides an approximately 10-fold higher resolution than light microscopy. The ability to study samples under ambient pressure with virtually no sample preparation allows aqueous systems to be studied. In addition, time-resolved microscopic studies can be carried out. Therefore, X-ray microscopy is a useful tool for the investigation of precipitation reactions. Recent results in instrumentation and applications of X-ray microscopy can be found in ref 6.

Current Knowledge Regarding $CaCO_3$ Precipitation. For better consideration of the results presented here, we will first summarize some aspects of structure formation in $CaCO_3$ precipitation reactions:

* To whom correspondence should be addressed. E-mail: jens.rieger@basf-ag.de. Phone: ++49 621 60 73731. Fax: ++49 621 60 92281.

† BASF Aktiengesellschaft.

‡ University of Göttingen.

(1) Matijevic, E. In *Chemical Processing of Advanced Materials*; Hench, L. L., West, J. K., Eds.; John Wiley: New York, 1992; p 513.

(2) Muramatsu, A.; Sugimoto, T. *J. Colloid Interface Sci.* **1997**, *189*, 167.

(3) Ocana, M.; Rodriguez-Clemente, A.; Sema, C. J. *Adv. Mater.* **1995**, *7*, 212.

(4) Cölfen, H.; Antonietti, M. *Langmuir* **1998**, *14*, 582.

(5) Rieger, J.; Hädicke, E.; Rau, I. U.; Boeckh, D. *Tenside, Surfactants, Deterg.* **1997**, *34*, 430.

(6) *X-ray microscopy and spectromicroscopy*; Thieme, J., Schmahl, G., Rudolph, D., Umbach, E., Eds.; Springer: Berlin, 1998.

10.1021/la0004193 CCC: $19.00
Published on Web 10/07/2000

(a) Owing to its importance, $CaCO_3$ precipitation has been studied for more than 100 years[7] both in basic research (biology, geology, mineralogy, chemistry) and in applications (fillers, pigments, encrustation). However, this precipitation is still far from understood, particularly regarding processes at a microscopic level.

(b) The thermodynamically stable crystal modification of $CaCO_3$ is calcite. In addition, $CaCO_3$ is known to have the two modifications vaterite and aragonite as well as the amorphous state and two hydrate forms.[8]

(c) As a typical example of Ostwald's step rule,[9] the first step in precipitation is the formation of $CaCO_3$ in the amorphous form, which at room temperature is preferentially converted into vaterite and finally into calcite. There is virtually no detailed or substantiated knowledge of the conversion mechanisms.[10]

(d) While calcite is usually recognizable from the rhombohedral crystal habit, the precursors frequently occur as beads having a diameter of up to a few micrometers.[11−14] Contradictory statements have been made regarding the intermediate structures. For example, it is asserted on one hand that the beads are spherolithically grown vaterite crystals.[10,15] It has furthermore been observed that these beads are initially in amorphous form and suddenly crystallize spherolithically from the inside outward to yield vaterite.[16] On the other hand, scanning electron photomicrographs of broken beads show that they consist of aggregated nanoparticles with diameters of about 50 nm.[11]

(e) These $CaCO_3$ nanoparticles seem to represent basic structural units under many precipitation conditions. They are not only the units from which our studies show that $CaCO_3$ beads are built up, but also interact with additives used to modify the precipitation (see below). The nanoparticles form; only then are they coated, for example, with polycarboxylate molecules, although the polymers have been present in the system since the beginning of the precipitation.[5]

(f) The existence of nanoparticles as basic units is also supported by wide-angle X-ray studies (WAXS), which, on evaluation of the line widths of precipitated $CaCO_3$, give values for the crystallite sizes in the region of 50 nm.

(g) The use of polycarboxylates employed as additives in detergents for inhibiting encrustation allows two polymer concentration ranges to be distinguished regarding the change in Ca^{2+} activity during the precipitation: in precipitations which correspond to the supersaturation conditions in very hard water, we observe a stepwise drop in Ca^{2+} activity after a few minutes at low polymer concentrations. At higher polymer concentrations (for example above a value of 150 ppm in the case of polycarboxylates, see below), the Ca^{2+} activity—after an immediate drop from the initial value (formation of $CaCO_3$ particles) in both cases—remains at a level which then stays constant. The structural causes for this effect have only now been explained by means of the X-ray microscopy studies described below.

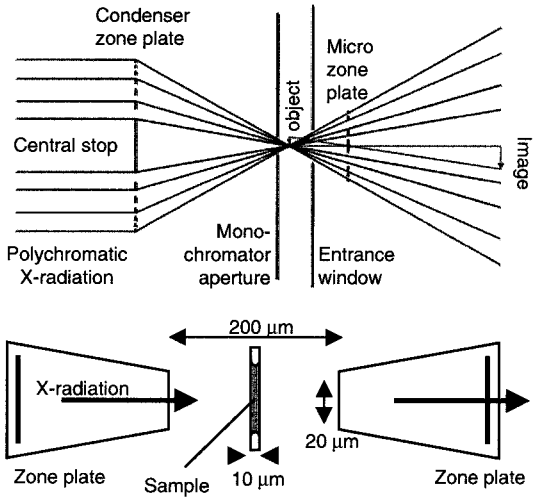

Figure 1. Optical setup of the X-ray microscope and sketch of the object area.

(h) Finally, it should also be pointed out that the product morphology in precipitation reactions is frequently extremely sensitive to the precipitation conditions and in particular to the way in which the starting solutions are mixed. For example, in experiments aimed at explaining the mechanisms of action of additives, precipitations with variation of defined parameters, for example the additive concentration, must as far as possible be carried out under otherwise identical conditions. This point should be kept in mind when comparing the results reported here with other investigations.

2. Experimental Section

2.1. X-ray Microscopy. X-ray microscopy, as used for these studies in the form of transmission X-ray microscopy (TXM), is an imaging method similar to light microscopy or transmission electron microscopy (TEM) with the advantages already mentioned above. For the studies described here a transmission X-ray microscope (TXM) has been used, which has been developed and is operated by the Institute for X-ray Physics at the University of Göttingen.[17] It utilizes synchrotron radiation of the electron storage ring BESSY I in Berlin. In the wavelength range between the K-absorption edge of oxygen at $\lambda = 2.34$ nm and carbon at $\lambda = 4.38$ nm radiation is weakly absorbed by water compared to the absorption within other organic or inorganic substances. This gives rise to a natural contrast in images of aqueous colloidal systems.

The optical setup of the X-ray microscope and a sketch of the object area are shown in Figure 1. Due to the high absorption within all materials and as the refractive index for these materials is very close to one, it is not possible to use refractive optics in the wavelength range mentioned above. Instead, zone plates are used as optical elements.[18] These are circular diffraction gratings with radially decreasing line widths. Figure 2 shows the center part of a zone plate made of germanium, which is used as a high-resolution X-ray objective. The width of the outermost zone determines the maximum resolution achievable with these optics. For the experiments described here the resolution is in the order of 40 nm.

The samples are prepared by placing one drop of the suspension to be studied on a 0.15 μm thin support foil. This foil consists of polyimide coated with a few nanometers thick layer of silicon and silicon dioxide. The drop is covered with a second foil of the

(7) Nancollas, G. H.; Reddy, M. M. *J. Colloid Interface Sci.* **1971**, *37*, 824.
(8) Clarkson, J. R.; Price, T. J.; Adams, C. J. *J. Chem. Soc., Faraday Trans.* **1992**, *88*, 243.
(9) Söhnel, O.; Garside, J. *Precipitation*; Butterworth-Heinemann: Oxford, U.K., 1992; p 145.
(10) Kabasci, S.; Althaus, W.; Weinspach, P.-M. *Trans. Inst. Chem. Eng.* **1996**, *74A*, 765.
(11) Rieger, J.; Frechen, T. Unpublished results.
(12) Söhnel, O.; Mullin, J. W. *J. Cryst. Growth* **1982**, *60*, 239.
(13) Ogino, T.; Suzuki, T.; Sawada, K. *Geochim. Cosmochim. Acta* **1987**, *51*, 2757.
(14) Brecevic, L.; Nielsen, A. E. *J. Cryst. Growth* **1989**, *98*, 504.
(15) Tracy, S. L.; Williams, D. A.; Jennings, H. M. *J. Cryst. Growth* **1998**, *193*, 382.
(16) Addadi, L. Personal communication.
(17) Niemann, B.; Schneider, G.; Guttmann, P.; Rudolph, D.; Schmahl, G. In *X-ray microscopy IV*; Aristov, V. V., Erko, A. I., Eds.; Bogorodski Pechatnik: Chernogolovka, Russia, 1994; p 66.
(18) Peuker, M.; Schneider, G.; Weiss, D. *SPIE Proc.* **1998**, *3449*, 118.

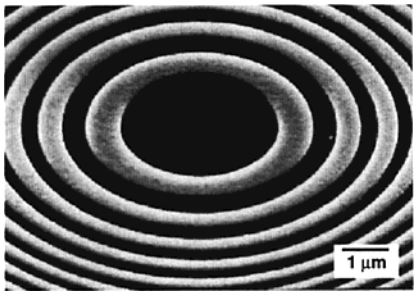

Figure 2. TEM image of the center part of a germanium zone plate.

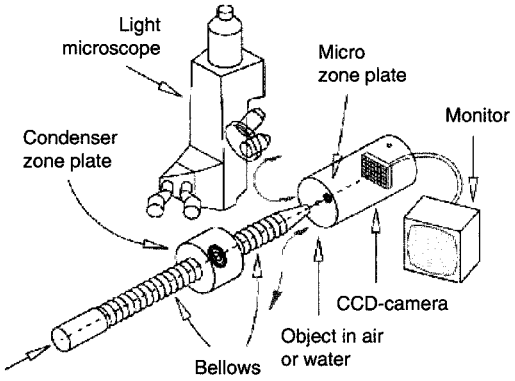

Figure 3. Design of the X-ray microscope used at BESSY I.

same type. It is then adjusted to a thickness of about 10 μm by applying a slight downward pressure.[17] The resultant sandwich is mounted in the beam path and adjusted by means of a light microscope. From commencement of preparation to the first exposure takes about 3 min if working quickly. An xy device allows an area of a few square millimeters to be studied. The object section visible at any one moment is 15 μm in diameter. The image data are read from a CCD camera and stored digitally for further processing.[19] The design of the TXM is shown in Figure 3. One aspect that needs particular attention in X-ray microscopy studies is possible damage to the sample by the intense X-ray beam. Organic samples are particularly susceptible. This point is checked by exposing comparable sample sections for different times and comparing the images obtained. Changes caused by the X-ray beam are evident from disappearance or new formation of structures or gas formation. In our experiments with exposure times in the region of a few seconds, beam damage was not observed.

Another point, which must be stressed, is that the temporal resolution of the experiments is given by the exposure time, which is in the order of 2−10 s. This means that it is not possible to detect single particles with a diameter of some tens of nanometers, which do not adhere to the surfaces of the confining foils. This is due the Brownian motion of these particles.

2.2. $CaCO_3$ Precipitation. Precipitation was initiated by mixing a 0.01 M Na_2CO_3 solution with a 0.01 M $CaCl_2$ solution in a Y-shaped mixing piece made out of glass. The flow rate was 1.5 mL/min per solution. The cross section of the flow channels was 5 mm. These concentrations were used in continuation of our earlier studies;[5] supersaturation of about 170 is obtained. When studying the mode of action of additives, the polymer was added to the Na_2CO_3 solution. An acrylic acid/maleic acid copolymer with a monomer ratio of 7:3 and an average molar mass of about 70000 g/mol was used in our experiments. This polymer is used as incrustation inhibitor in laundry detergents.

3. Results

3.1. $CaCO_3$ Precipitation without Additives. Figure 4 shows a typical result when $CaCO_3$ is precipitated without addition of additives. First, beads measuring less than 1 μm form. The beads dissolve in the course of time, and the intergrown crystals shown in Figure 5 form. Both photographs were taken of the same sample in the X-ray microscope.

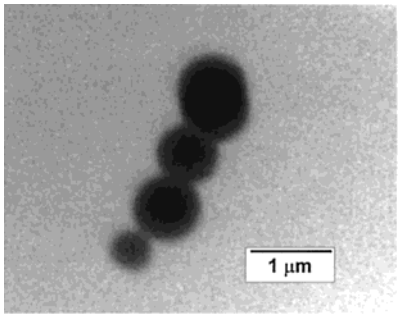

Figure 4. $CaCO_3$ particles in the aqueous phase in the case of precipitation without additives after 4 min.

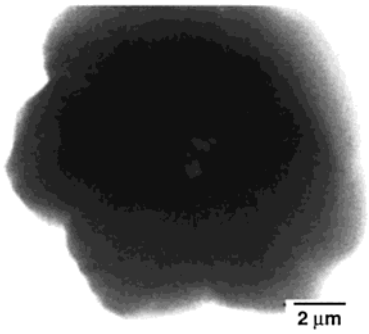

Figure 5. $CaCO_3$ particles in the aqueous phase in the case of precipitation without additives after 45 min.

The fact that solution and crystallization effects can indeed be observed here with time resolution is due to the capability for the system to be studied in the aqueous phase. The only restriction is the layer thickness of 10 μm. Any $CaCO_3$ particles with a size of up to some dozen nanometers cannot be detected as they cannot be imaged owing to Brownian motion of the particles at an "exposure time" of a few seconds.

Our previous findings on the $CaCO_3$ precipitation process obtained using WAXS and electron diffraction indicate that the beads are $CaCO_3$ in amorphous form or in the vaterite structure. The crystals forming are in the thermodynamically stable calcite modification. We attribute the fact that there is no formation of rhombohedra, as are typical of calcite, to crystallization taking place in a restricted geometry. The dimensions of the object in Figure 5 are already in the order of the film separation; i.e., diffusion of the ions forming the crystal takes place differently from that in the unrestricted three-dimensional case. The restriction of the space by the cover films also seems to be responsible for the pale region in the center of the crystal object in Figure 5; this position is presumably occupied by the crystal nucleus, which, as we know from further TXM images (Figure 6), is frequently localized on the surface of one of the beads of the type that can be seen in Figure 4. Since on one hand the beads dissolve during recrystallization and since on the other hand calcite has already formed around this area, a region of low density is left behind.

The process of dissolution of the $CaCO_3$ beads that form initially can for the first time be followed in detail with time resolution using a TXM, as documented in Figure 7. It can be seen how the beads increasingly lose contrast in the aggregate until they disappear completely. Interest-

(19) Wilhein, T.; Rothweiler, D.; Tusche, A.; Scholze, F.; Meyer-Ilse, W. In *X-ray microscopy IV*; Aristov, V. V., Erko, A. I., Eds.; Bogorodski Pechatnik: Chernogolovka, Russia, 1994; p 470.

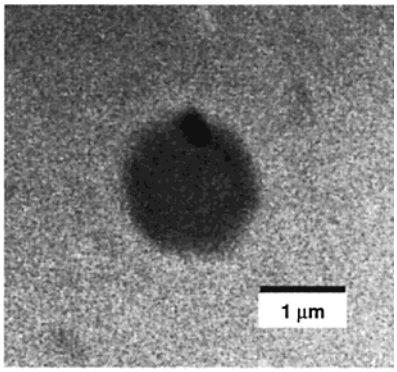

Figure 6. $CaCO_3$ precursor with nucleus at the "North Pole" a few minutes after commencement of precipitation.

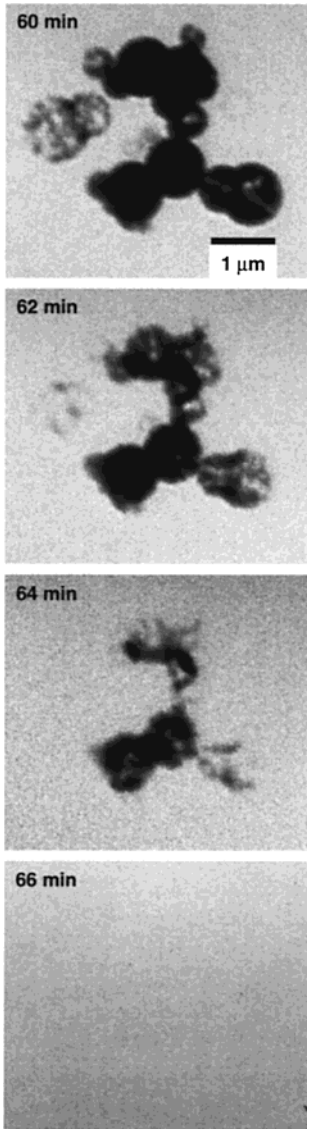

Figure 7. Dissolution process of $CaCO_3$ particles in the aqueous phase. The times indicated correspond to the time interval from commencement of the precipitation by mixing.

ingly, the dissolving beads have a granular structure with dimensions in the region below 100 nm. It is at present impossible to say whether these are inhomogeneities in the beads (for example regions of varying hydration), which could have formed due to density fluctuations during the actual precipitation process, or precursor nanoparticles of $CaCO_3$, which form the observed beads by aggregation and "cementing". This point is discussed again in a different context below.

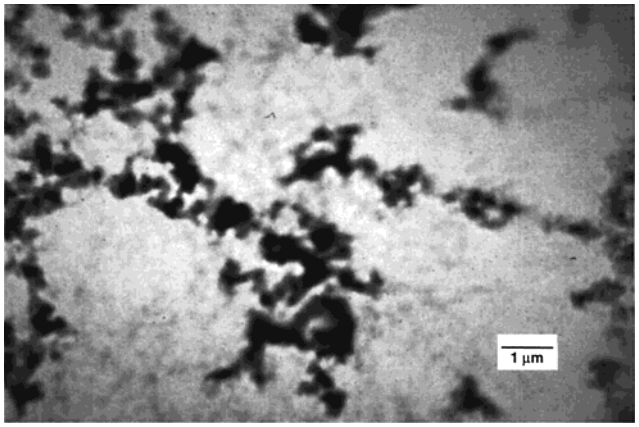

Figure 8. Result (in the aqueous phase) of a $CaCO_3$ precipitation ($Na_2CO_3 + CaCl_2$) in the presence of 200 ppm of polycarboxylate (see text).

The fact that the dissolution of the beads is not an artifact caused by radiation damage has been shown by a comparison of regions of the overall sample exposed to different amounts of radiation.

One reason the dissolution phenomenon observed here is so interesting is that it had previously not been possible to explain clearly how the conversion into the stable calcite modification proceeds. For example, it was not clear how long the diffusion paths of the ions are during recrystallization. Figures 4−7 show that the metastable modification actually dissolves completely without a nucleus of the more stable phase in the immediate vicinity. The ions of the dissolved structure in general diffuse for more than 10 μm before they recrystallize to form calcite. The driving force for this process is the difference in chemical potential of the various structures. The fact that a thermodynamically unfavorable modification initially forms corresponds to Ostwald's step rule.[9]

The apparent inconsistency of the times indicated in Figures 5 and 7 needs explanation. In Figure 5, calcite has formed after only 45 min and does not change further in its dimensions, while the dissolution process documented in Figure 7 only commences after 60 min. The time scale is relatively unsharply defined in the present investigations, since supersaturation fluctuations which are difficult to estimate seem to occur. The cause of this is first that the separation between the substrate and cover films cannot be set to exactly the same value in all places and second because of the quasi-two-dimensionality of the system.

Finally it must be annotated that we observed a totally different behavior as regards the occurring structures when slightly changing the mixing conditions toward more turbulent mixing.[5] A shower of nanoparticles is to be seen. This apparent discrepancy will be discussed below.

3.2. $CaCO_3$ Precipitation in the Presence of Polycarboxylate. In a first experiment, 400 ppm of polycarboxylate was added to the Na_2CO_3 solution before the precipitation, so that 200 ppm was present in the precipitated system. The results of the precipitation are shown in Figure 8. Nanoparticles of $CaCO_3$ with a diameter of less than 100 nm are evident. These nanoparticles are in some cases aggregated and in addition embedded in a faint network. The nature of this network can be seen in Figure 9. For this photograph, the "precipitation experiment" was carried out without Na_2CO_3; i.e., only complex formation between carboxyl groups of the polymers and

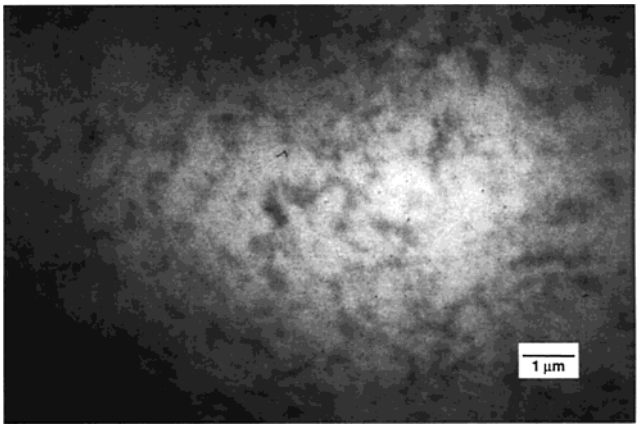

Figure 9. Result (in the aqueous phase) of a complexing reaction between polycarboxylate and Ca^{2+}. The experiment is as for Figure 8, but without Na_2CO_3.

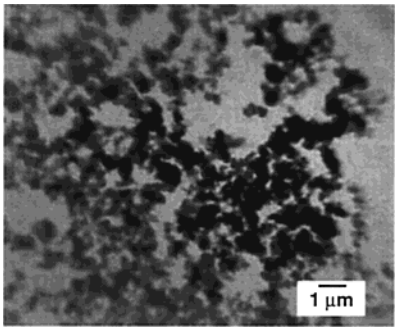

Figure 10. Result (in the aqueous phase) of $CaCO_3$ precipitation in the presence of 50 ppm of polycarboxylate. Time from commencement of the precipitation: 16 min.

Ca^{2+} ions can take place and particle formation is not expected. Figure 9 shows a network of the same type as the underlying network in Figure 8. This network obviously consists of polymer chains bridged by Ca^{2+}.

The formation of $CaCO_3$ nanoparticles embedded in a network of bridged polymers has already been postulated in an earlier paper[5] on the basis of indirect evidence, namely the following findings: (a) macroscopic flocculation (visible finding); (b) flocs contain nanoparticles (transmission electron microscopy); (c) polymers are found in the serum (analytical ultracentrifuge), i.e., not all polymers are bound to the surface of the nanoparticles; (d) pure polycarboxylate can be flocculated by means of Ca^{2+} (visible finding). X-ray microscopy now makes it possible to render this structure visible for the first time.

It should be noted that the structure does not change over the course of time at the selected polymer concentration (200 ppm of polycarboxylate); i.e., the nanoparticles are stabilized.

A different precipitation mechanism is observed if less polymer is used. On precipitation in the presence of 50 ppm of polycarboxylate, i.e., at a batch concentration of 100 ppm in the Na_2CO_3 solution, the structure shown in Figure 10 is formed initially. This structure is similar to that formed on use of the higher polymer concentration. In contrast to the previous case, however, this structure is *not* stable: Figure 11 shows the *same* image section as Figure 10. It can be seen that the structure has dissolved. The liberated ions crystallize at a different sample location in a form similar to that which we have already observed as the end result of precipitation without additives (Figure 12). The rounded form compared with Figure 5 may be due to the effect of the polymer on the crystallization process.

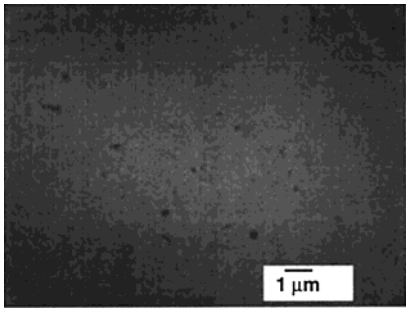

Figure 11. Result (in the aqueous phase) of $CaCO_3$ precipitation in the presence of 50 ppm of polycarboxylate. Time from commencement of the precipitation: 48 min. *This is the same image section as in Figure 10.*

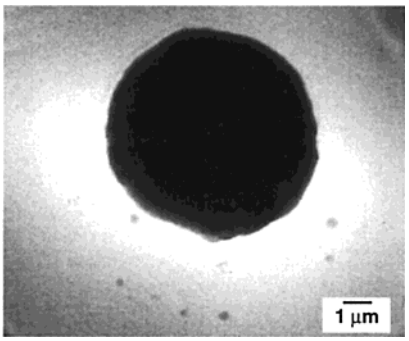

Figure 12. Result (in the aqueous phase) of $CaCO_3$ precipitation in the presence of 50 ppm of polycarboxylate. Time from commencement of the precipitation: 58 min. This image section is different from the one in Figure 10.

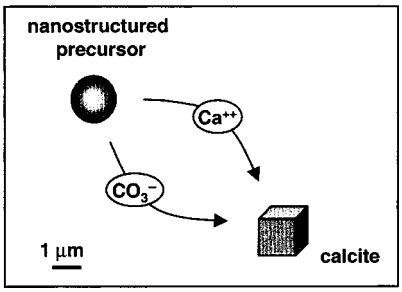

Figure 13. Schematic representation of the processes taking place during precipitation of $CaCO_3$ without additives (in the concentrations used here): Dissolution of (nanostructured) precursors and recrystallization to give calcite.

When 50 ppm of polycarboxylate is present in the precipitating system, the number of polymers is apparently insufficient to stabilize the nanoparticles. A rough calculation shows that the amount of carboxyl groups provided by the polymer is in this case not sufficient to cover the surfaces of the nanoparticles. The fact that there is a critical polymer concentration which is necessary to stabilize nanoparticles efficiently against dissolution by coating has likewise already been postulated in earlier papers on the basis of indirect findings.[5] Using X-ray microscopy, the phenomenon can—again for the first time—be rendered visible with time resolution on the length scale of the nanoparticles.

4. Discussion

The findings described here on $CaCO_3$ precipitation and the effects of polycarboxylate on the precipitation are shown schematically in Figures 13−15.

Precipitation without Additives. See Figure 13. The following points may be made: (a) First, beads having

dimensions up to some micrometers form; according to earlier studies, these precursors are in amorphous form or in the vaterite modification. (b) These precursors dissolve, and the ions diffuse over a distance of several micrometers and then recrystallize (on suitable nuclei) in the thermodynamically stable calcite modification according to earlier studies. (c) On dissolution of the beads, a granular structure is evident; whether this structure is attributable to buildup of the beads by aggregation of nanoparticles can only be assumed on a basis of the available data. However, earlier studies give indications in support of this hypothesis. Likewise, the observation that $CaCO_3$ nanoparticles can be stabilized by additives supports the hypothesis that nanoparticles are formed as primary units at the beginning of the precipitation. (d) Another point that must be kept in mind is the fact that little is known about the composition of the initial particles. Assuming that these are highly hydrated amorphous, one might speculate whether some spinodal decomposition process is involved.

Point a above (formation of precursor structures in the region of a few micometers) is known from the literature, while the phenomena described under points b−d were observed by us for the first time in this form.

It has been stressed already that due to Brownian motion it is not possible to image colloidal particles, which do not adhere to the surfaces of the confining foils. Thus we cannot judge whether free $CaCO_3$ nanoparticles are involved in the processes discussed so far. Results from cryo-TEM experiments on quenched $CaCO_3$ precipitations clearly demonstrated the existence of such nanoparticles.[5] Also, the precipitation experiments in the presence of polycarboxylates hint at the existence of such colloidal particles. A point that needs further consideration is the influence of the condition of mixing. The importance of this point must not be underestimated.[20] It might be speculated whether the mild mixing conditions of the present experiments resulted initially in a quite inhomogeneous system where the nucleation occurred at the interface between the two reacting solutions. This in turn might have led to the spheres, which have been observed. The occurrence of nanoparticles in turn might be due to a more perfect mixing yielding a more uniform supersaturation. But still in the case of turbulent mixing it is an open question where nucleation actually takes places, at the interface in turbulent eddies or in a perfectly homogeneous system. Obviously, this point needs further attention.

Precipitation with Polycarboxylate. The following points may be made: (a) The precipitating $CaCO_3$ nanoparticles are initially fixed in a network of polymers (Figure 14). (b) If the amount of polymer is sufficient to cover the surface of the nanoparticles completely, the nanoparticles remain in this form (Figure 15). (c) If the amount of polymer is not sufficient, the nanoparticles dissolve, and the ions recrystallize elsewhere (Figure 15)—again in the thermodynamically stable calcite modification in accordance with our studies.

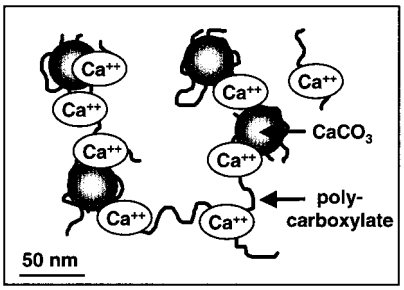

Figure 14. Schematic representation of the processes taking place during precipitation of $CaCO_3$ in the presence of polycarboxylates: Fixing of $CaCO_3$ nanoparticles in a network of polymers bridged by Ca^{2+}.

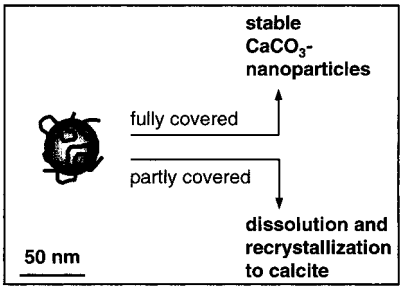

Figure 15. Given adequate coating of the $CaCO_3$ nanoparticles by polymers, the nanoparticles are retained. With inadequate coating, they dissolve, and the ions recrystallize to give micometer-sized calcite crystals.

Of course, more work is needed in order to fully understand all the details of $CaCO_3$ precipitation. For example, it will be interesting to vary the concentrations of the salt solutions used or to include "inert" electrolyte to affect electrostatic interactions. The limited beamtime available for the present studies prevented us from performing these experiments.

In conclusion, we have shown that X-ray microscopy is a suitable technique for studying the morphological evolution in precipitation/crystallization reactions. The main advantage of this method is the possibility to achieve time and space resolved information with minimal interference with the ongoing processes. An important drawback is obviously the lack of sensitivity for particles with dimensions up to some dozens of nanometers, which evade detection because of Brownian motion. For the system studied, i.e., $CaCO_3$ precipitation, the occurrence and dissolution of precursors was visualized directly. The effect of polycarboxylates on the precipitation could be followed in real time on a length scale below 100 nm. The observations allowed for an understanding of the mode of action of these additives with respect to the formation and stabilization of $CaCO_3$ nanoparticles.

LA0004193

(20) Baldyga, J.; Bourne, J. R. *Turbulent Mixing and Chemical Reactions*; Wiley: New York, 1999.